Gene expression divergence between locally adapted inland annual and coastal perennial ecotypes of *Mimulus guttatus* across developmental stages

Running title: Ecotypic gene expression divergence

Jason D. Olsen[a,b] Billie A Gould[a] Yani Chen[a] and David B. Lowry[a,b,c,*]

[a]Department of Plant Biology, Michigan State University, East Lansing, MI, USA 48824

[b]Ecology, Evolution, and Behavior, Michigan State University, East Lansing, MI, USA 48824

[c]Plant Resilience Institute, Michigan State University, East Lansing, MI, USA 48824

*Correspondence should be addressed to D.B.L. (dlowry@msu.edu)

Key Words: Auxin, Gibberellin, Hormone, Jasmonic Acid, Reproductive Isolation, Transcription

ABSTRACT

The action of natural selection across heterogeneous natural landscapes drives local adaptation and the formation of plant ecotypes, the precursors to new species. Plant ecotypes typically differ significantly in morphology, physiology, and development, yet our understanding of their underlying genetic basis remains limited. Despite their importance, studies of the molecular underpinnings of ecotypic divergence through developmental stages are rare. Here, we compared gene expression at different developmental time points between ecologically reproductively isolated coastal perennial and inland annual ecotypes of the yellow monkeyflower, *Mimulus guttatus*. We took two major approaches to understand differences in gene regulation between the ecotypes at the level of gene networks. First, we evaluated expression variation between the ecotypes in candidate molecular pathways. Next, we conducted gene co-expression network analyses to identify new candidate mechanisms driving ecotypic divergence. Overall, we found significant differences in global expression between the ecotypes and across developmental stages. Among the candidate pathways we evaluated, genes in the jasmonic acid pathway were the most significantly enriched for divergent gene expression. This includes the most differentially expressed gene in our analyses, which is a key gene (cytochrome P450 CYP94B1) involved in the degradation of bioactive jasmonic acid. Our gene co-expression network analysis revealed different but complementary insights into the differential regulation of genes between the ecotypes, especially at a more microscopic level of these organisms. Overall, our research further supports the hypothesis that plant hormone pathways play a crucial role in the evolution of plant ecotypes and, consequently, the emergence of new species.

INTRODUCTION

The evolution of new species generally occurs over long periods of time and involves a combination of geographic isolation, natural selection, and genetic drift (Coyne & Orr 2004). In plants, speciation is thought to often be facilitated through ecogeographic isolation among populations driven by local adaptation (Schemske 2000; Sobel et al. 2010; Sobel 2014; Butlin & Faria 2024). This process leads to the formation of ecotypes, which initially are reproductively isolated by ecological isolating barrier (Lowry 2012; Butlin & Faria 2024). These ecotypes generally have higher fitness in their native habitats, which limits gene flow between habitats and, in turn, facilitates the buildup of greater divergence and reproductive isolating mechanisms (Sobel et al. 2010; Lowry 2012). In this way, ecotypes can be viewed as intermediates in the process of speciation.

Some of the greatest progress in our understanding of the evolution of plant ecotypes comes from studies of the adaptive divergence between coastal and inland plant ecotypes. Indeed, Turesson's (1922a,b) ecotype concept was largely inspired by the high level of morphological divergence between coastal and inland populations of plants in Sweden. Clausen, Keck, and Hiesey famously followed up on the work of Turesson through multiple monograph-length studies of coastal and inland ecotypes of multiple plant species in California (Clausen et al. 1940, 1948). Since that time, several other researchers have found similar patterns of differentiation between coastal and inland ecotypes worldwide (Boyce 1954; Nagy & Rice 1997; Foster et al. 2007; Verhoeven et al. 2008; Itoh et al. 2024). From these studies, some major generalizations can be made about ecotypic differentiation associated with coastal habitats (Lowry 2012). Coastal ecotypes are generally more dwarfed in stature, prostrate in their growth form, and

flower later than inland ecotypes of the same species. Boyce (1954) argued that much of this growth form difference was due to coastal plant adaptations to oceanic salt spray, and suggested that coastal ecotypes might be better referred to as salt spray ecotypes.

While the concept of plant ecotypes was first formulated by Turesson (1922a,b) over a century ago, our understanding of the genetic, physiological, and developmental mechanisms underlying the evolution of ecotypes remains limited. Some of the largest advances in our understanding of ecotype evolution have come from the coastal ecotype systems, where molecular genetic and genomic tools have recently become available. For example, recent molecular research on the evolution of dune and headland populations of *Senecio latifolius* on the east coast of Australia has revealed many clues about the evolution of plant ecotypes (Roda et al. 2013; James et al. 2021, 2023; Wilkinson et al. 2021; Broad et al. 2024). In *S. latifolius*, the headland ecotype experiences intense winds, and presumably salt spray, which in combination with the availability of steep cliff habitat has driven a dwarfed and prostrate growth architecture. In contrast, the dune ecotype is taller with an upright growth habit, which may reflect a more sheltered habitat where this growth form is advantageous. Recent genetic research on this system suggests a complex genetic basis of the differences in physiology and development between the dune and headland ecotypes. Despite this complexity, there is strong evidence for a role of evolutionary changes in the auxin hormone pathway being involved in the changes in growth form, especially with a large divergence in gravitropism between the ecotypes (Wilkinson et al. 2021; James et al. 2023; Broad et al. 2024).

Given the major role that plant hormone pathways play in shaping the growth form and physiology of plants, it is perhaps not surprising that they may also play a key role in the evolution of plant ecotypes (Voesenek & Blom 1996; VanWallendael et al. 2019; Broad et al. 2024). Recent research has shown that hormone pathways interact with each other through complex crosstalk through which they coordinate development and stress responses (Fujita et al. 2006; Depuydt & Hardtke 2011; Murphy 2015; Aerts et al. 2021; Gasperini & Howe 2024). For example, the jasmonic acid and gibberellin hormone pathways are thought to coordinate plant trade-offs between growth and defense at least partially through the interaction of JASMONATE ZIM-domain (JAZ) and DELLA genes in each of these hormones' respective signaling pathways (Pieterse et al. 2014; Howe et al. 2018; Guo et al. 2018). While we are still far from understanding the highly complex network of plant hormone interactions, our current knowledge of these pathways provides great utility for gaining new insights into how plant ecotypes evolve through local adaptation to different habitats.

To better understand how hormone and other key pathways have shifted in the evolution of plant ecotypes, we conducted a study of gene expression divergence between coastal and inland ecotypes through developmental stages, from the first set of true leaves to the emergence of floral buds. The focus of our study was on coastal and inland ecotypes in the yellow monkeyflower, *M. guttatus*. Over the past two decades, extensive research has been conducted to understand the evolutionary mechanisms underlying the divergence of inland annual versus coastal perennial ecotypes in this species (Hall et al. 2006, 2010; Lowry et al. 2008, 2009; Lowry & Willis 2010; Twyford & Freidman 2015; Twyford et al. 2015; Gould et al. 2017, 2018; Popovic & Lowry 2020; Kollar et al. 2025). There are large differences in a wide swath of traits

113 between coastal perennial and nearby inland annual ecotypes (Abrams 1951; Hitchcock and
114 Cronquit 1973; Vickery 1978; Lowry et al. 2008). These ecotypes diverge in traits such as
115 growth rate, morphology, phenology, and resistance to herbivory, and are locally adaptative in
116 reciprocal transplant experiments (Hall and Willis 2006; Van Kleunen 2007; Lowry et al. 2008;
117 Hall et al. 2010; Lowry et al. 2019). In general, the inland annual ecotype flowers early to avoid
118 seasonal drought and produces fewer true leaves before developing floral buds. The coastal
119 perennial ecotype flowers later and produces more leaf pairs before budding. Based on the
120 morphological distinctness of the coastal perennial ecotype, some taxonomists have raised it to
121 the species level, naming it the magnificent monkeyflower, *Mimulus grandis* (syn. *Erythranthe*
122 *grandis*; Nesom 2012). However, given the high level of allele sharing between coastal perennial
123 and inland annual groups of populations (only four fixed nucleotide differences out of >29
124 million SNPs; Gould et al. 2017), we more cautiously treat each group as an ecotype instead of a
125 species. While we don't consider the coastal perennial and inland annual ecotypes as distinct
126 species, we do recognize that they are on the speciation continuum, as they have acquired a
127 significant level of ecologically-based reproductive isolation (Lowry et al. 2008; Lowry & Willis
128 2010).
129
130 Prior research on the coastal perennial and inland annual ecotypes suggests that their
131 morphological divergence is largely driven by evolutionary shifts in hormone pathways. This
132 hypothesis first emerged as a result of a prior population genomic outlier study (Gould et al.
133 2017), which identified genes in the gibberellin hormone pathway as top candidate genes for
134 ecotype divergence. One of those candidate genes, GA20ox2, a key enzyme in the gibberellin
135 biosynthetic pathway, is located in a chromosomal inversion polymorphism on chromosome 8

136 that is responsible for a substantial portion of the divergence between coastal perennial and
137 inland annual ecotypes (Lowry & Willis 2010; Friedman 2014; Lowry et al. 2019; Blanchard et
138 al. 2024). A recent study found that GA20ox2 is not expressed in leaves; however, it exhibits
139 higher expression in the shoot apices of inland annuals compared to coastal perennials (Kollar et
140 al., 2025). This differential expression could initiate a developmental cascade that impacts the
141 expression of other important pathways in developing leaves, branches, and reproductive
142 structures, which may explain some of the broad phenotypic effects associated with the
143 chromosome 8 inversion. Indeed, the application of gibberellin (GA3) to coastal perennial plants
144 leads to substantial phenotypic changes, converting their growth architecture from prostrate to
145 upright (Lowry et al. 2019) and making them more susceptible to oceanic salt spray in the field
146 (Toll et al. 2024). Beyond its significant morphological and phenological effects, the
147 chromosome 8 inversion also contributes to elevated constitutive and inducible levels of
148 defensive phenylpropanoid glycoside (PPG) in coastal perennials versus inland annual plants
149 (Lowry et al. 2019; Blanchard et al. 2024). This finding suggests the involvement of the
150 jasmonic acid (JA) hormone pathway in the differentiation of coastal and inland plants, as PPG
151 production is known to be stimulated by jasmonic acid. Given the known cross-talk between the
152 gibberellin and jasmonic acid pathways (Fujita et al. 2006; Yang et al. 2012; Wasternack 2017;
153 Züst & Agrawal 2017; Guo et al. 2018), evaluation of expression patterns for gene in those
154 pathways could provide further insights into the mechanisms underlying the divergence of the
155 ecotypes.
156
157 In this study, we analyzed patterns of gene expression between coastal perennial and inland
158 annual accessions of *M. guttatus* across development, from the production of the first pair of true

159 leaves to the emergence of floral buds. The primary goal of this work was to understand how
160 coastal perennial and inland annual ecotypes are differentiated at the level of gene networks. To
161 that end, we took two complementary approaches. First, we evaluated how individual genes were
162 differentially regulated between ecotypes and across developmental stages, across all of the
163 major plant hormone pathways. Based on our prior work, we hypothesized that the gibberellin
164 and jasmonic acid pathways would have an elevated level of differential gene expression
165 between the ecotypes. In addition to hormone pathways, we evaluated gene expression in the Salt
166 Overly Sensitive (SOS) pathway, as a few key genes in this pathway were implicated in
167 divergence between the ecotypes in prior work (Gould et al. 2018). Following our analyses of
168 individual genes in candidate pathways, we conducted a whole-genome transcriptional module
169 analysis using a Weighted Gene Co-expression Network Analysis (WGCNA; Langfelder and
170 Horvath 2008). This analysis did not incorporate any prior knowledge about the *M. guttatus*
171 system and was thus effective at generating additional new hypotheses of mechanisms
172 underlying divergence of the ecotypes. Overall, we found that the two approaches to
173 understanding gene expression at the network level provided different, yet complementary,
174 insights into ecotype divergence.
175

176 **METHODS**

177 **Plant material**

178 To identify patterns of gene expression divergence between the ecotypes, we selected one coastal
179 perennial (SWB-4) and one inland annual (LMC-17) accession for a detailed study throughout
180 development. The coastal perennial SWB population (N 39.02.159, W 123.41.428) is located near
181 Manchester, CA, while the inland annual population LMC (N 38.51.839, W 123.05.035) is located

182 near Boonville, CA. By focusing on two accessions, we were able to achieve a high level of
183 replication for each developmental stage. Seeds from each accession consisted of self-fertilized
184 families that were two generations inbred in the laboratory before the experiments. To eliminate
185 potential maternal effects, seeds were grown for one additional generation at Michigan State
186 University (MSU, East Lansing, MI) in the four months before the growth chamber experiment,
187 where tissue was collected for gene expression analysis.

188 **Plant growth conditions**

189 Surface-sterilized *Mimulus guttatus* seeds were placed on 60 mm diameter x 15mm height Petri
190 dishes containing half-strength Linsmaier and Skoog (LS) medium: 1.5% w/v sucrose and 0.25%
191 Phytagel (P8169, Sigma, St. Louis, MO). Seeds were then stratified at 4°C in the dark for 14 days.
192 After cold treatment, plants were germinated at 20°C under a 16 h 100 mE light / 8 h dark cycle for 5
193 to 14 days in a Percival (Percival Scientific, Perry, IA) chamber. Cotyledon-stage seedlings were
194 transferred to 3.5-inch square pots containing SureMix Perlite (Michigan Grower Products,
195 Galesburg, MI) and grown in a BioChambers FXC-19 flex growth chamber (BioChambers,
196 Winnipeg, Manitoba) in the same conditions as in the Percival chamber. Three key steps were taken
197 to minimize the effects of environmental heterogeneity within the growth chamber. First, the
198 locations of plants were fully randomized across trays within the chamber. Second, the tray position
199 within the chamber was haphazardly rotated daily. Third, the developmental stage at which each
200 plant was sampled was assigned randomly. Leaf pairs and floral buds were collected in a time series
201 (Fig. S1). Leaves were collected at the point in development when they were nearing maximal
202 expansion. The floral buds were collected from plants around the time of anthesis. Only one tissue
203 was collected per plant to avoid induced responses and repeated measures. Each tissue collection was
204 harvested in a fixed time window (14:00 to 14:30) during the simulated daylight period. Tissue was
205 immediately flash frozen on liquid nitrogen and stored in a -80° C freezer. RNA was later extracted

206 from samples using a Spectrum Plant Total RNA Kit (Sigma-Aldrich, St. Louis, MO). We collected
207 10 biological replicates for each developmental stage x ecotype combination (*N* = 80 total tissue
208 samples). For the inland annual plants, we sampled at the two-leaf, four-leaf, and floral bud stages
209 because plants often flowered after producing two pairs of true leaves. Because the coastal perennial
210 plants flowered at a later developmental stage, we sampled at the two-leaf, four-leaf, six-leaf, eight-
211 leaf, and floral bud stages. All tissue samples were collected before anthesis.

212 **Library preparation and sequencing, and processing**

213 We prepared genomic libraries using a 3'-Tag-Seq procedure, which restricts sequencing to the 3' end
214 of mRNAs and dramatically reduces the cost for RNA-seq studies (Meyer et al. 2011; Lohman et al.
215 2016; Marx et al. 2020). Our protocol for library preparation followed an updated version of the
216 methods of Meyer et al. (2011), which had been adapted for sequencing on the Illumina platform, as
217 described in Weng & Juenger (2022). The detailed protocol of library preparation for our study can
218 be found in the Supplemental Methods. Each sample was assigned a fully randomized position across
219 four pools of 20 samples before library construction. The MSU Genomics Core Facility conducted
220 sequencing in Illumina HiSeq 2500 Rapid Run flow cells (v2) in the 1x100bp conformation.
221 Sequencing of the four pooled libraries was conducted across three different flow cells, with two
222 pools being sequenced in two separate flow cells and the other pools only being sequenced on a
223 single flow cell each.
224
225 Raw Illumina reads were processed following our protocol that is available on GitHub along with
226 code for other analyses detailed below
227 (github.com/lowrylab/Mimulus_expression_across_development). Briefly, raw reads were first
228 examined for quality with FastQC (bioinformatics.babraham.ac.uk/projects/fastqc/), which found a
229 median Phred score of ~37 across libraries. Adapter sequences were then removed with Cutadapt

230 (Martin 2011). Cutadapt was applied with an adapter mismatch error threshold of 20% of primer
231 length. Primer trimming began with the 5' end (NNNN followed by 3-5 G's with a first step to cut 8
232 bases and a second step to cut the remaining 5' G's). Trimming of the 3' end was done by removing
233 15bp of the 3' end of each read to remove the poly-A primer and any readthrough. To retain only
234 high-quality sequences after trimming, any bases on either end with a quality score < 30 were
235 removed, and we required the last two bases of each read to match the poly-A primer while
236 discarding any reads <30bp in length. These parameters align with the requirements for the Tag-Seq
237 methodology to remove both adapter sequences and non-template bases created during library
238 preparation (Meyer et al. 2011). Trimmed sequence files were concatenated and aligned to the
239 *Mimulus guttatus* v2.0 reference genome (Hellsten et al. 2013; phytozome-next.jgi.doe.gov) using
240 the memory-efficient Burrows-Wheeler Aligner (BWA-MEM; Li 2013), as in Marx et al. (2020) and
241 Weng & Juenger (2022). The v2.0 reference genome was selected for alignment because genes are
242 well annoatated and it has been used for many other recent studies. Aligned reads were filtered to
243 include only high-quality, primary alignments using Samtools 1.2 (Li et al. 2009). The total number
244 of aligned reads retained for each sample was calculated with Samtools. Counting the number of
245 reads aligned per gene per sample was done with HT-seq v.0.6.1 (Anders et al. 2015) with "stranded"
246 and "union" parameter options. Count files were filtered to remove genes with < 5 aligned reads to
247 exclude non-expressed genes or alignment artifacts.

248 **Clustering analyses of gene expression**

249 To evaluate whether samples clustered based on genotype, developmental stage, and/or library pool,
250 we conducted a principal component analysis (PCA) with DESeq2 (Love et al. 2014) in R version
251 4.4.2. Before the implementation of normalization and PCA, we filtered out low abundance genes by
252 removing any genes did not have more than 10 counts in more than 5 samples. We then normalized
253 the remaining data using a variance stabilizing transformation (VST). The PCA was conducted with

254 this filtered and normalized data (Fig. 1). We focused on the top two PCs, as they explained far more
255 of the variation than any of the other PCs (Fig. S2). In addition to the PCA, we evaluated clustering
256 of the same VST data with a heat map produced by the R pheatmap function.
257
258 **Differential gene expression analyses at the individual gene level**
259 To evaluate differential expression analyses at the individual gene level, we used the edgeR-voom-
260 limma framework (Law et al. 2014), implemented in R version 4.5.0. Voom-limma was selected for
261 this analysis because it stabilizes the mean-variance relationships of count data for linear modeling
262 and allows for complex experimental designs with multiple interactions. Our analysis of differential
263 gene expression focused on the 2-Leaf, 4-Leaf, and bud developmental stages, as inland annual
264 plants generally did not produce 6-Leaf and 8-Leaf tissue. Prior to model fitting, we filtered the raw
265 count data using the filterByExpr function, which is part of the edgeR package (version 4.6.1;
266 Robinson et al., 2010). This function retains only genes that have sufficient counts to achieve
267 statistical significance through differential expression analysis, using the default parameters. We used
268 version 3.64.0 of limma for this analysis. Normalization was then conducted for count data using the
269 calcNormFactors function, which accounts for composition bias and library size differences. This
270 normalized data was then converted to log2-counts per million (log2-CPM) using the voom
271 transformation.
272
273 The following linear model was fit for each gene:
274
275 expression ~ genotype + development_stage + genotype:development_stage
276

277 Empirical Bayes methods were used to shrink gene-wise variances, which improves the reliability of
278 inference for genes with highly variable transcript abundance. The "Inland" genotype and "2leaf"
279 developmental stage were set as the reference levels for statistical contrasts. We tested for differential
280 expression of genes for five contrasts: 1) Main effect of genotype (Coast vs. Inland), 2) main effect
281 of developmental stage for 4leaf vs. 2leaf), 3) main effect of developmental stage for bud vs. 2leaf, 4)
282 interaction between genotype and developmental stage for 4leaf vs. 2leaf, and 5) interaction between
283 genotype and developmental stage for bud vs. 2leaf. We controlled for multiple testing by calculating
284 False Discovery Rate (FDR) adjusted *P*-values using the Benjamini-Hochberg method. To evaluate
285 how closely overall gene expression analyzed with the voom-limma approach mirrored the analysis
286 of all genes using DESeq2, we output a multidimensional scaling (MDS) plot for the 2leaf, 4leaf, and
287 bud stages.
288

289 **Analysis of candidate pathways**

290 To evaluate whether any hormone pathways were enriched for differentially expressed genes, we
291 examined the expression of core genes involved in hormone pathways. These core pathway genes for
292 each of the major hormone pathways (Table 1) were identified by custom Python scripts to parse the
293 *Mimulus guttatus* v2.0 genome annotation file. Gene lists identified by these scripts were further
294 refined through close inspection, followed by the removal of genes of lower confidence. We used the
295 gene lists that we compiled for those pathways to extract the gene expression results for each gene
296 from our individual gene analyses (above). Once we had identified the number of differentially
297 expressed genes (FDR adjusted $P < 0.05$) and highly differenitally expressed genes (Log-Fold
298 Change (LFC) > 2), we tested for enrichment with Fisher-Exact tests, with Benjamini-Hochberg FDR
299 adjusted correction for multiple testing. In addition to hormone pathway genes, we also evaluated
300 key genes in plant cellular homeostasis, including genes in the Salt Overly Sensitive (SOS) pathway,

301 given prior evidence that these genes may be important for coastal adaptations in this system (Gould
302 et al., 2017, 2018). As with the hormone pathway genes, we used custom python scripts to identify
303 candidate genes from the v2.0 annotation file.
304
305 **Gene co-expression module analyses**
306 To identify gene co-expression modules across genotypes and developmental stages, we conducted a
307 Weighted Gene Co-expression Network Analysis (WGCNA; Langfelder and Horvath 2008). As
308 with the analysis of candidate pathways, we focus this analysis on the 2leaf, 4leaf, and bud
309 developmental stages. Before network construction, we re-conducted a VST normalization with
310 DESeq2 in R version 4.5.0. To improve the signal in the data, we filtered out low-expressed genes
311 with fewer than 10 counts in fewer than 5 samples. Following WGCNA recommended best
312 practices, we used a scale-free topology model fit of $R^2 > 0.80$. To minimize the influence of
313 outliers, biweight midcorrelations were used instead of Pearson correlations. We used dynamic
314 tree cutting with a minimum module size of 30 genes and deepSplit parameter of 2 to identify
315 modules. We then merged similar modules that had correlations among module eigengenes,
316 representing the first principal component of each module, of greater than 0.75. Module
317 membership of genes was established through correlations between gene expression and the
318 eigengene of each module. We defined candidate hub genes for each module as the top ten genes
319 with the highest module membership.
320
321 To interrogate the functional significance of each identified module, we conducted a GO
322 enrichment analysis of genes within each module using an annotation file from the *Mimulus*
323 *guttatus* v2.0 genome. Here, enrichments analyses of GO terms were performed using a
324 hypergeometric test of a comparison of lists of genes in each module to all annotated genes using

325 a Benjamini-Hochberg FDR for multiple testing. We also closely inspected the annotations of hub
326 genes to further understand the functional significance of each module.
327

328 **RESULTS**

329 **Sequencing and alignment**

330 Overall, sequencing resulted in a total of 343,561,167 raw reads. Across the 80 samples, there
331 was a minimum of 4,271,651 reads and a maximum of 10,858,583 reads (median of 7,403,646
332 reads per sample). We identified 28,140 unique gene transcripts.
333

334 **Clustering analyses of gene expression**

335 For the PCA, we retained 18,054 genes after filtering for low expression. The PCA (Fig. 1) of the
336 prefiltered, VST-normalized expression values for these transcripts revealed a distinct grouping
337 of samples along two major axes. Comparing gene expression through development between the
338 coastal perennial and inland annual ecotypes of *M. guttatus* is challenging, as these ecotypes
339 often develop at different rates and put on different numbers of leaves before flowering. Both *M.*
340 *gutatus* ecotypes go through two-leaf and four-leaf vegetative stages. However, the inland
341 ecotype often flowers at the next node after the 4-leaf stage, while the coastal ecotype transitions
342 through 6-leaf and 8-leaf stages before forming floral buds. Despite this concern, there was a
343 high level of clustering across all leaf stages for both the coastal perennial and the inland annual
344 plants in the PC analysis (Fig. 1). PC1 corresponded most closely to differences between leaf and
345 bud tissue and accounted for 53.4% of the expression variance. PC2 corresponded to the
346 divergence between the coastal and inland ecotype samples and accounted for 19.8% of the

347 variance. The heat map visualization results were consistent with our PCA results, and also revealed

348 that there was no clustering of samples based on the library pool (Fig. S3).

349

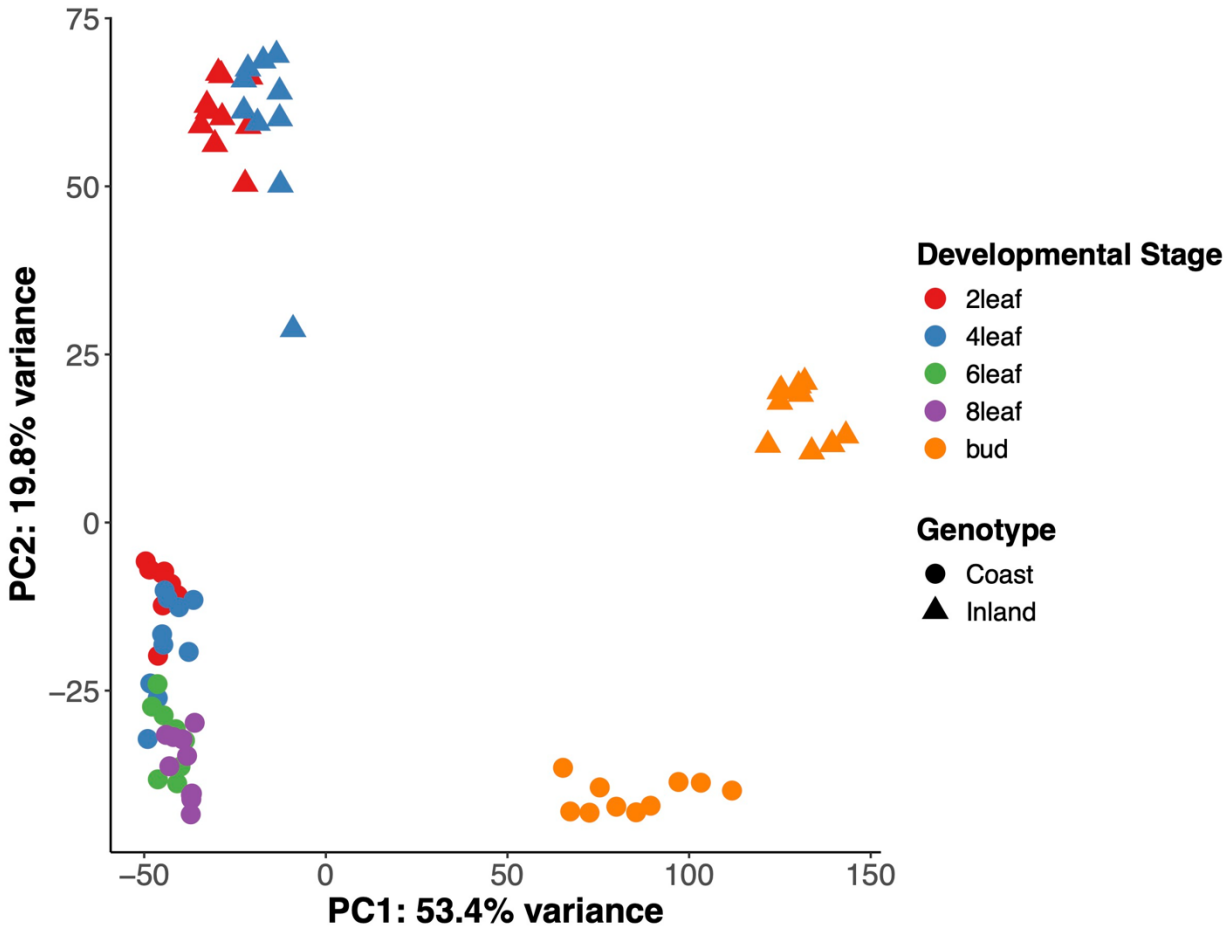

Figure 1: Principal component analysis of pre-filtered, variance-stabilizing transformed (VST) transcript count data from RNASeq. Different colors denote all combinations of developmental stages and ecotypes. The first principal axis (PC1) explains the variance in the dataset and primarily distinguishes differences between leaf (vegetative) and bud (reproductive) stages. The second principal axis explains the variance that primarily distinguishes differences between ecotypes.

350

351 **Differential gene expression analyses at the individual gene level**

352 Analysis of individual gene expression using the EdgeR-voom-limma approach revealed

353 numerous significantly differentially expressed genes for the five major contrasts derived from

354 linear modeling (Figs. S3-S7). After filtering by the filterByExpr function, 13,920 genes were

355 retained for statistical analyses. Of these, the following numbers of genes were significantly

356 differentially expressed with a Benjamini-Hochberg adjusted *P*-value of <0.05: 7238 genes were
357 differentially expressed for the main effect of genotype (Coast vs. Inland), 2398 for the main effect of
358 developmental stage (4leaf vs. 2leaf), 10,248 for the main effect of developmental stage (Bud vs.
359 2leaf), 886 for the interaction between genotype and developmental stage for 4leaf vs. 2leaf, and
360 5337 for the interaction between genotype and developmental stage for bud vs. 2leaf. For the
361 genotype main effect, 3417 genes had significantly higher expression in inland annual plants, while
362 3821 genes had significantly higher expression in coastal perennial plants. Complete gene lists with
363 statistical results can be found in the supplementary materials. MDS visualization of the 2-leaf, 4-
364 leaf, and bud stages for 13,920 genes retained after filtering (Fig. S9) revealed a strikingly similar
365 ordination of samples to the PCA for all samples (Fig. 1).
366

367 **Analysis of candidate pathways**

368 Across the nine hormone pathways, we identified 768 candidate genes using the v2.0 annotation
369 (Table 1). Of those, 351 genes were expressed at a high enough level for individual gene
370 analyses (above), with 195 differentially expressed between the ecotypes (genotype main effect).

Table 1: Differential gene expression of hormone pathway genes between coastal and inland ecotypes and between the floral bud and second pair of true leaves (2-leaf) developmental stages.

Hormone Pathway	Candidate Genes	Genes Evaluated	Ecotype DE	Ecotype LogFC > 2	Bud vs 2-Leaf DE	Bud vs 2-Leaf LogFC > 2
Gibberellin	64	19	12	4	14	6
Jasmonic Acid	82	49	40***	23***	35	15
Abscisic Acid	102	64	27	1	42	14
Brassinosteroid	49	29	16	1	20	5
Auxin	271	111	60	8	90	27
Cytokinin	99	38	23	2	23	4
Ethylene	61	28	14	1	23	5
Salicylic Acid	27	6	1	1	5	0
Strigolactone	13	7	2	0	3	1
Genome-wide	28140	13920	7238	926	10248	2347
***Significant enrichment at an FDR adjusted P<0.001						

371 There were 41 highly differentially expressed (LFC>2) hormone genes, of which 35 were in the
372 auxin, gibberellin, or jasmonic acid hormone pathways. The jasmonic acid pathway genes in
373 particular were overrepresented for differential expression (FDR adjusted $P = 0.00027$) and

374 highly differential expression (FDR adjusted $P = 2.6x10^{-13}$) between the coastal and inland

375 ecotypes. While the gibberellin pathway was overrepresented for highly differentially expressed

376 genes, the pattern was not significant after FDR adjustment.

377

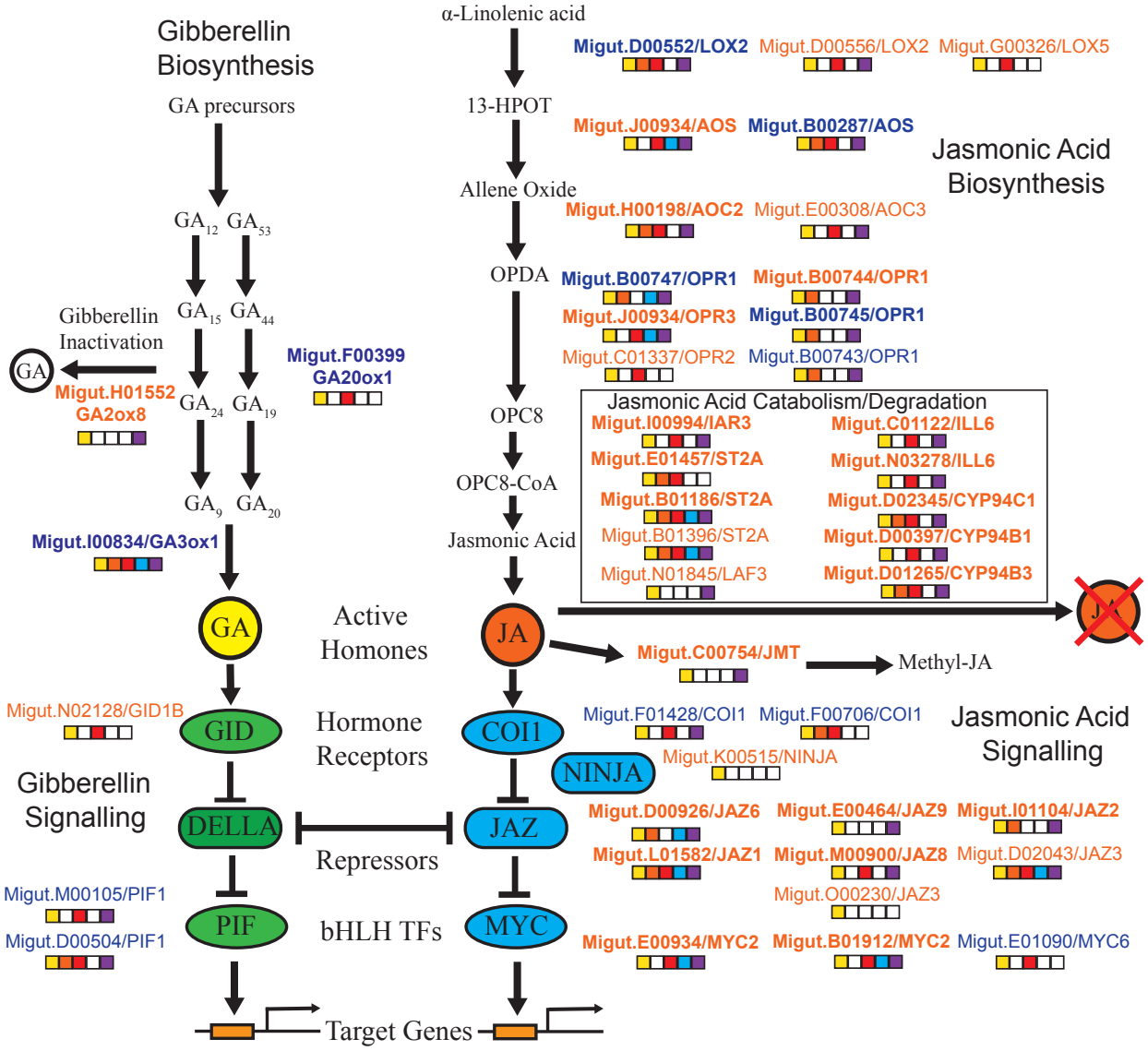

Figure 2: Gene expression patterns for the candidate gibberellin (GA) and jasmonic acid (JA) biosynthetic and signaling pathways. Genes that were significantly differentially expressed between coastal and inland plants (genotype main effect, yellow filled square) are shown. The names of genes with higher expression in inland plants are indicated with orange letters, while genes with higher expression in coastal plants are indicated by blue letters. Other significant contrasts are also indicated by filled squares: 4leaf vs. 2leaf (orange), bud vs. 2leaf (red), genotype interaction with 4leaf vs. 2leaf (blue), and genotype interaction with bud vs. 2leaf (purple). Bolded gene names indicate LFC > 2 for the genotype main effect.

378 Because of our a priori hypothesis about the role of the gibberellin and jasmonic acid pathways

379 in divergence of the coastal and inland ecotypes, we evaluated differentially expressed genes in

380 the context of their position in the biosynthetic and signaling pathways for these hormones (Fig.
381 2). Striking patterns of gene expression were observed across the core GA and JA pathway genes
382 (Fig. 2). In the jasmonic acid pathway, all seven of the differentially expressed (genotype main
383 effect) *JAZ* genes in the signaling pathway and all ten of the differentially expressed JA
384 catabolism/degradation genes had higher expression in inland plants than coastal plants. In
385 contrast, the two orthologs of the *COI1* (coronatine-insensitive protein 1) were downregulated.
386 *COI* and *JAZ* genes are co-receptors of bioactive jasmonic acid-isoleucine (JA-Ile; Monte et al.
387 2022). In the gibberellin pathway, genes promoting GA biosynthesis (*GA20ox1* and *GA3ox1*)
388 were upregulated in coastal plants, while the only differentially expressed gene involved in GA
389 inactivation (*GA2ox8*) was upregulated in inland plants. In the GA signaling pathway, an
390 ortholog of the gibberellin receptor *GID1B* was upregulated in inland plants, while two
391 phytochrome-interacting factor (*PIF1*) orthologs were upregulated in coastal plants. The only
392 *DELLA* gene in *M. guttatus* (Migut.H02266) was not significantly differentially expressed
393 between the genotypes. However, this *DELLA* gene was differentially expressed between the bud
394 and 2-leaf developmental stages (LFC = -3.17; adjusted $P = 8.49 \times 10^{-9}$), with higher expression
395 in leaves than in buds.
396
397 For each of the other hormone pathways, we report which genes were highly differentially
398 expressed (LFC >2) here: Eight auxin genes were highly differentially expressed, including two
399 orthologs of *ILL6* (Migut.C01122, Migut.N03278), an ortholog of *ILL3* (Migut.F00137), an
400 ortholog of *SHY2* (Migut.N02182), and four auxin-responsive genes (Migut.F01336,
401 Migut.F01339, Migut.F01341, and Migut.N01563). Only one brassinosteroid candidate gene was
402 highly differentially expressed, a *BRI1* kinase inhibitor 1 (*BKI1*; Migut.N02706), which had

403 greater expression in inland plants. The two highly differentially expressed cytokinin genes were
404 orthologs of *ARR12* (Migut.K00347) and *APRR7* (Migut.L01650). The one highly differentiated
405 abscisic acid gene was an *ABA4* ortholog, which had greater expression in coastal plants. The
406 only differentially expressed salicylic acid gene, a *Mov34/MPN/PAD-1* family protein
407 (Migut.O00742), was also highly differentially expressed. There was only one highly
408 differentially expressed ethylene gene, an ortholog of an ethylene responsive element binding
409 factor 1 (*ERF1*; Migut.O00367).
410

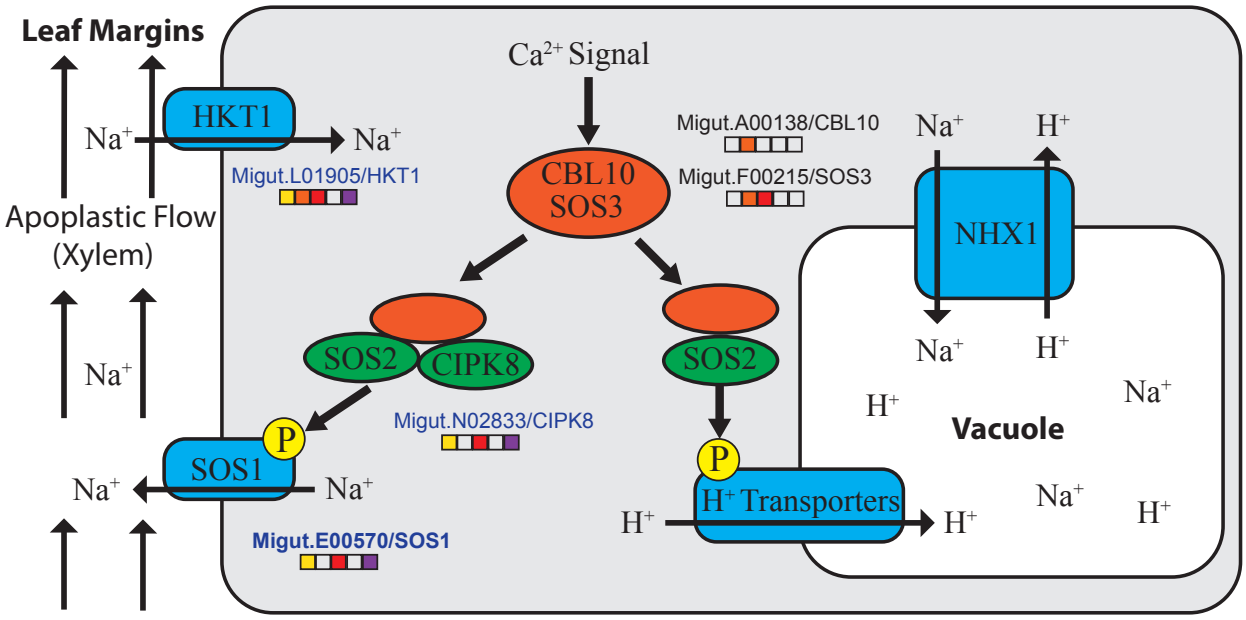

Figure 3: Expression of genes involved in sodium homeostasis. Model of cellular sodium homeostasis genes. *CBL10* and *SOS3* play similar roles in propagating the calcium signal resulting from salt stress, but their roles differ across cell types. Genes significantly differentially expressed between coastal and inland plants (genotype main effect) are indicated by yellow-filled squares. Names of genes with higher expression in coastal plants are indicated by blue letters. Other significant contrasts are also indicated by filled squares: 4leaf vs. 2leaf (orange), bud vs. 2leaf (red), genotype interaction with 4leaf vs. 2leaf (blue), and genotype interaction with bud vs. 2leaf (purple). Bolded gene names indicate LFC > 2 for the genotype main effect.

411 For genes involved in sodium homeostasis, we identified 15 high-confidence candidate genes. Of
412 these, only five were expressed at a high enough level for individual gene statistical analyses
413 (Fig. 3). Three of those genes were significantly expressed between the coastal and inland plants
414 (genotype main effects): Orthologs of *SOS1* (Migut.E00570), *HKT1* (Migut.L01905), and *CIPK8*
415 (Migut.N02833). Only *SOS1* had an LFC greater than 2 (Fig. 3, 4).

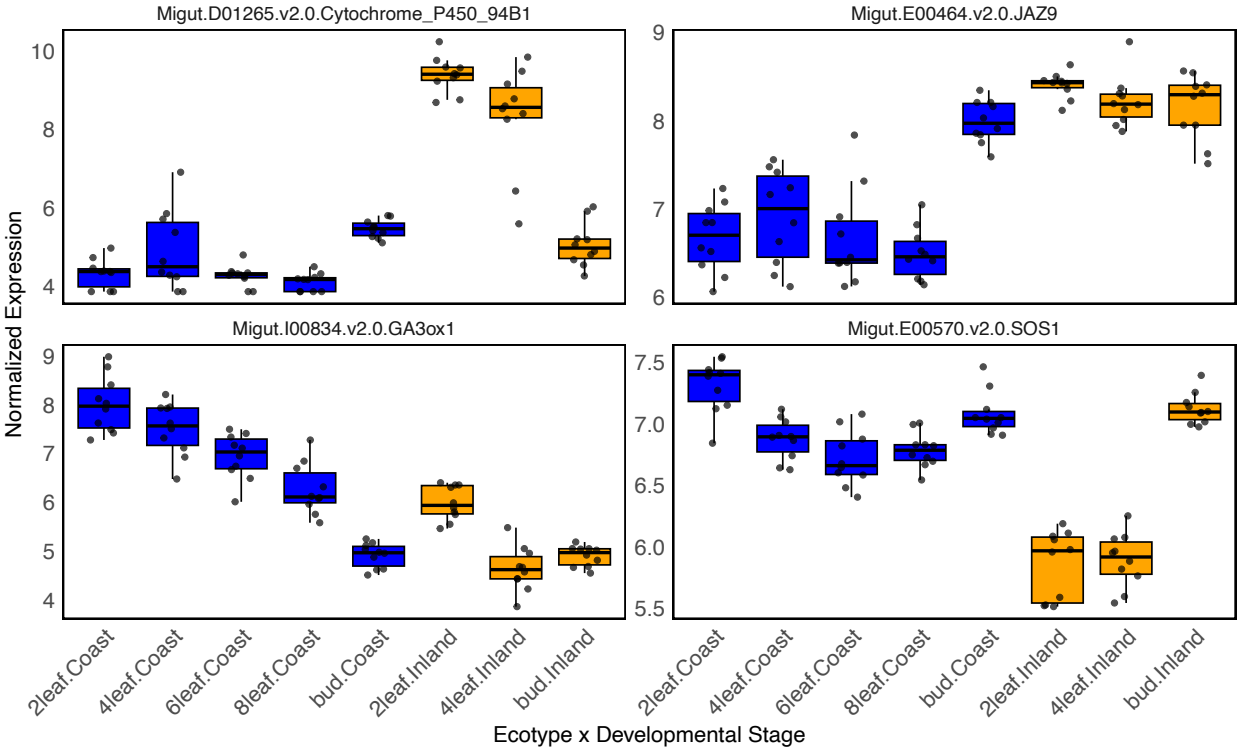

Figure 4: Ecotype x developmental stage interactions in gene expression. Patterns of expression for four candidate genes through developmental stages that had LFC > 2 for the contrast between the genotypes. Cytochrome P450 94B1 is the first gene in the jasmonic acid degradation pathway. JAZ9 is one of the key regulatory genes in the jasmonic acid signaling pathway. GA3ox1 is an important gibberellin biosynthesis gene. SOS1 is the key gene that pumps sodium from the cytoplasm of plant cells into the apoplast. Gene expression in the plot was VST normalized.

416

417

418

419

420

421

Gene co-expression module analyses

Analyses with WGCNA revealed nine major gene co-expression modules after the merging of correlated modules. The following number of genes were assigned to each module: red = 2315, tan = 1874, turquoise = 4937, green =1686, black = 2633, cyan =184, lightcyan = 62, blue =3131, greenyellow = 1232. The eigengenes of each of these modules were differentially correlated with genotype and developmental stage (Figure 5; Fig. S10-S27).

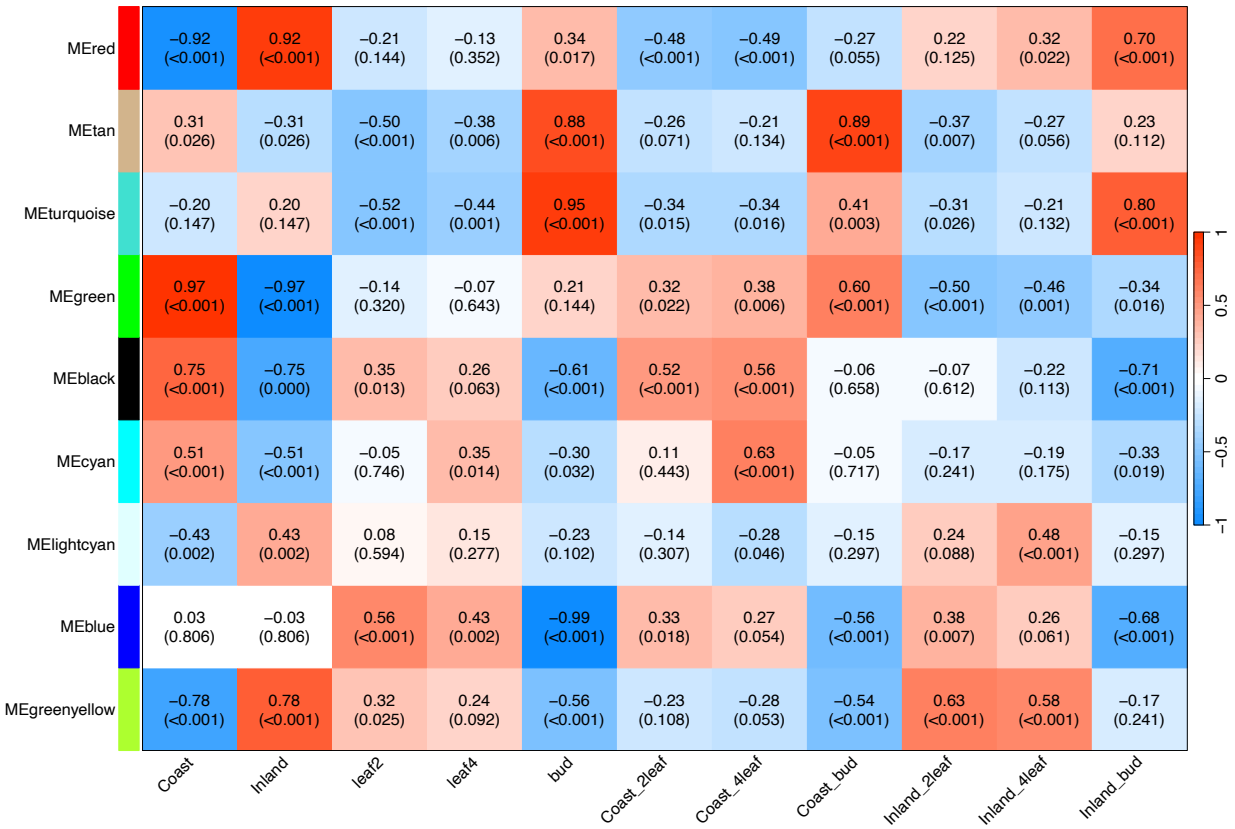

Figure 5: Gene co-expression module correlations with ecotype and developmental stages. The correlation between the eigengene of each module with ecotype, stage, and ecotype x stage combinations are reported above FDR adjusted *P*-values.

429 Gene Ontology (GO) enrichment
430 analysis, combined with an
431 examination of the functions of hub
432 genes, revealed distinct potential
433 functions for each of the nine modules.
434 The modules that most differentiated
435 the coastal and inland genotypes were
436 the green, red, greenyellow, and black
437 modules. The green module appears to
438 differentiate coastal and inland plants
439 in stress responses and cell death
440 decisions. The red module appears to
441 be primarily associated with vesicle
442 trafficking and membrane dynamics.
443 The greenyellow module is likely
444 involved in the coordination of growth
445 and stress responses, with auxin
446 biosynthesis and signaling potentially
447 playing a key role. One of the hub genes in the greenyellow module is a key auxin gene, *Amidase 1* (Migut.F01717).
448
449

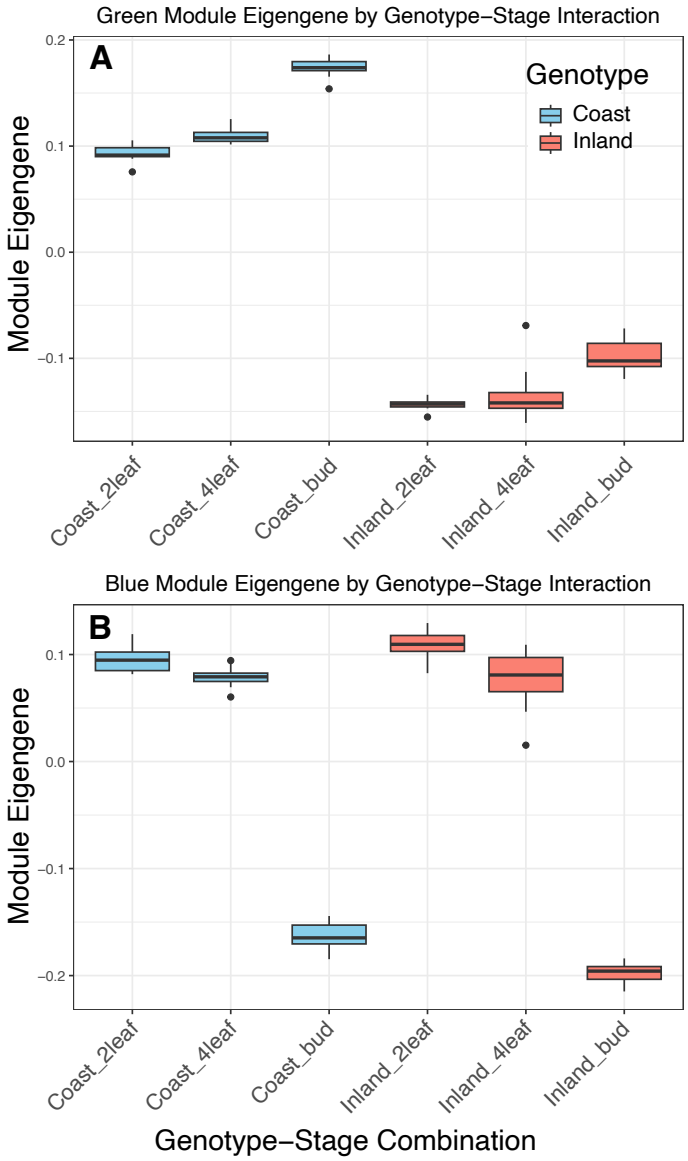

Figure 6: Ecotype x developmental stage of co-expression modules. (A) The green module contained genes that principally differed between the ecotypes. (B) The blue module genes were primarily differentially expressed between leaves and floral buds.

450 The cyan and lightcyan modules were differentiated between the ecotypes at the leaf stages, but

451 less differentiated at the bud stage (Fig. 5, S15, S16). Based on the gene composition of the

Table 2: Hypothesized biological function and list of key hub genes for each of the nine modules identified by WGCNA analyses.

Module	Biological function prediction based on GO enrichment and hub genes	Key hub genes
Red	Vesicle trafficking and membrane dynamics, with a possible roles in stress responses. Coordinates phospholipid signaling, vesicle formation, membrane identity, and trafficking processes	Phospholipase D (PLD; Migut.B01671), an important signaling molecule that promotes membrane curvature and facilitates vesicle fusion and fission. Sec1/munc18-like (SM) protein (Migut.E01133), which is involved in vesicle trafficking. Nudix hydrolase 19 (Migut.J01169), which is a regulator of cellular redox homeostasis, crucial for plant stress responses.
Tan	Coordination of plant hormone responses with metabolism, lipid synthesis, posttranslational modifications, and cell wall remodeling. Likely important in growth and development.	Cellulase glycosyl hydrolase (Migut.A00708) and sucrose phosphate synthase (Migut.E01808) are involved in coordination between sugar metabolism and cell wall remodeling. Three of the hub genes were hormone genes involved in jasmonic acid biosynthesis (OPR1, Migut.B00746), gibberellin response (Migut.E01377), and auxin signaling (GH3, Migut.N02078).
Turquoise	Cell wall modifications, membrane dynamics, secretory pathway function, and cell surface signaling/environmental responses.	A pectin methylesterase inhibitor (Migut.C00970) that controls cell wall rigidity. A pectin lyase protein (Migut.M00012) that breaks down pectin in cell walls. EHD1 (Migut.H01794), a gene that regulates endocytic recycling. Two arabinogalactan proteins (AGP20 (Migut.F00245), AGP12 (Migut.K00009)), which are cell surface glycoproteins involved in signaling.
Green	Involved in balancing protein quality control and programmed cell death regulation. May be involved in acting as a molecular switch to determine whether stressed cells recover or undergo apoptosis.	Metacaspase 9 (Migut.K00195), a key protease that executes programmed cell death. A defender against death (DAD) protein (Migut.A01174). Galactinol synthase 2 (Migut.B00857), a gene involved in producing osmoprotectants to abiotic stress. A MADS-box transcription factor (Migut.K00994) that may play a key role in orchestrating stress responses and/or developmental impacts of the module.
Black	Ribosome biogenesis, RNA processing, and protein folding, likely serving as a hub for protein production and cellular growth.	Seven genes with ribosomal structure and function (Ribosomal L38e (Migut.F01852), S19 (Migut.G00718), S12/S23 (Migut.J00403), L35Ae (Migut.L01988), S8e (Migut.M01688), L14p/L23e (Migut.N02225), ans L1p/l10e (Migut.D02448). A peptidyl-prolyl isomerase (Migut.B00563) involved in protein folding. A cell cycle controlling cyclin (Migut.L00181).
Cyan	Enriched for microtubule processes, cell cycle regulation, chromosome dynamics, genome stability, and cytokinesis. Likely involved in plant growth and development through mitotic cell division and cell differentiation.	Microtubule and kinesin motor proteins (Migut.H01772, Migut.F00327). TPX2 (Migut.M00163), which is essential for spindle assembly. A cyclin-dependent kinase (Migut.C00348). Histone H2A6 (Migut.D02117) and a DNA methyltransferase (CMT3, Migut.D02536).
Lightcyan	Likely plays a central role in rapid responses to biotic stresses through pathogen/herbivore resistance and oxidative stress management.	Two MLP-like defense proteins (MLP423, Migut.N00310, Migut.N00312) involved in pathogen recognition/response. A serine protease inhibitor (Migut.A00978) involved in protection against herbivore and pathogen proteases. A peroxidase superfamily protein (Migut.J00066). An auxin responsive protein (Migut.H01293).
Blue	Chloroplast function and photosynthesis, including with both photosystems (I and II), light harvesting complexes, and thylakoid membrane components. The module also is involved in protein folding and redox homeostasis.	A PsbP-like protein 1 (PPL1, Migut.B00505), which is a component of photosystem II. A chloroplast stem-loop binding protein (CSP41A, Migut.D00296). DnaJ/Hsp40 molecular chaperone (Migut.K00479). Ascorbate peroxidase 4 (APX4; Migut.C00083), an antioxidant enzyme. Three chloroplast ribosomal genes (RPL9, Migut.D02295.1; RPL4, Migut.N00890.1; S5, Migut.H01481).
Greenyellow	Auxin response and metabolism, sulfur transport, redox homeostasis, protein structure/stability, and defense compound synthesis. Likely involved in the coordination of growth and stress responses.	Amidase 1 (AMI1; Migut.F01717), which converts indole-3-acetamide to active auxin. Heat stable protein 1 (HS1; Migut.N00022), which protects proteins during heat stress. FAD/NAD(P)-binding oxidoreductase (CTF2A; Migut.A01046). MLO (Migut.G00795), a transmembrane protein involved in defense responses.

452 lightcyan module, it appears to be involved in early stress responses, including plant biotic stress

453 defense and oxidative stress management. The cyan module is likely involved in cell division

454 and differentiation, and thus may play a key role in regulating plant growth.

455

456 Modules most associated with the developmental transition between leaf and floral bud included

457 the blue, tan, and turquoise modules. The blue module had much greater expression in leaves

458 than buds (Fig. 5, 6, S17) and was enriched for genes involved in photosynthesis. The tan and

459 turquoise modules both are likely involved in the developmental transitions through changes in
460 the expression of genes involved with the construction of cell wall and other processes.
461

462 **DISCUSSION**

463 In this study, we evaluated gene expression divergence between a coastal perennial and an inland
464 annual accession of *M. guttatus* during development. Overall, there were clear patterns of
465 differentiation between ecotypes and across developmental stages, with large shifts between leaf
466 and floral bud stages. Our analysis of gene expression in candidate pathways revealed a striking
467 elevation in differential expression between the ecotypes for genes in the jasmonic acid hormone
468 pathway, with expression patterns in that pathway consistent with the known divergence in
469 growth, reproduction, and defense between the coastal perennial and inland annual ecotypes.
470 While no other candidate pathways had significantly elevated expression differentiation, the
471 patterns of expression for some of the key genes in those pathways were informative. In contrast
472 to our candidate pathway analyses, the weighted gene network analyses revealed only limited
473 evidence for a role of plant hormone pathways in the divergence of the ecotypes. Instead, these
474 network analyses primarily revealed significant differences in cellular division, differentiation,
475 function, and growth between the ecotypes and across various developmental stages. These
476 differences at the microscopic level may ultimately help to give rise to organismal-level
477 divergence of the ecotypes, but have yet to be evaluated in detail in this system. By further
478 elucidating the mechanisms of ecotype formation, our work brings us closer to understanding the
479 complex changes involved in the evolution of ecogeographic and phenological reproductive
480 isolation.
481

482 **Gene regulatory divergence and the evolution of ecotypes**

483 The finding of elevated gene expression divergence for genes in both the jasmonic acid
484 biosynthesis and signalling pathways is a key result of our study. The higher gene expression of
485 the full complement of genes involved in JA catabolism/degradation in inland annual plants
486 suggests that jasmonic acid is not degraded across all stages at a high rate in the coastal perennial
487 ecotype, while JA may be quickly degraded and recycled in the leaves of the inland ecotype. Key
488 candidate genes, such as *CYP94B1*, exemplify this overall pattern. CYP94B1 is responsible for
489 the first step of degradation of bioactive jasmonic acid (Koo et al. 2014) and was the single most
490 differentially expressed gene (out of 13,920) between the ecotypes genome-wide (LFC = - 9.09;
491 Fig. 3; Supplementary Information). The coastal ecotype had a low expression level that was
492 consistent across all developmental stages. In contrast, the inland annual plants had a 40X higher
493 expression at the two-leaf stage but had a similar level of expression to the coastal ecotype in the
494 floral bud stage (Fig. 4). This pattern of gene expression suggests that jasmonic acid is not
495 degraded at a high rate across all stages in the coastal perennial ecotype while JA may be quickly
496 degraded and recycled in the leaves of the inland ecotype. Similarly, most of the genes in the
497 jasomic acid signalling pathway were expressed in a pattern consistent with previous studies that
498 found a higher production of defensive compounds in the leaves (Fig. 4) of perennial than annual
499 *M. guttatus* populations (Holeski et al. 2013; Lowry et al. 2019; Blanchard et al. 2024).
500

501 Trade-offs between rapid growth and herbivore resistance have long been recognized by plant
502 biologists. However, it is only recently that the underlying molecular mechanisms of such trade-
503 offs have begun to be elucidated. The gibberellin pathway is often seen as being at odds with the
504 jasmonic acid pathway in terms of regulating the trade-off between growth and herbivore defense

505 (Fujita et al. 2006; Yang et al. 2012; Züst & Agrawal 2017). An important recent discovery in
506 this area is that the gibberellin and jasmonic acid hormone pathways directly interact in an
507 antagonistic manner though the DELLA-JAZ signaling node (Kazan & Manners 2012; Havko et
508 al. 2016; Wasternack 2017). If this antagonistic interaction were driving trade-offs between
509 growth and defense in *M. guttatus*, we would expect a higher level of gibberellin activity in the
510 leaves of inland plants. This does not appear to be the case, as the pattern of gene expression in
511 the gibberellin pathway suggests more gibberellin biosynthesis and activity of the pathway in
512 coastal plants than inland plants. While most of the gibberellin candidate genes were not
513 expressed at a high enough level for individual gene analyses, the candidate genes in the
514 biosynthesis pathway all suggested a higher level of gibberellin biosynthesis, especially in leaf
515 tissues (Fig. 2, 4)
516
517 This finding of both higher gibberellin and jasmonic acid pathway activity in coastal leaves may
518 at first seem contradictory, except that it fits with our general understanding of how trade-offs
519 occur in this system. Coastal plants allocate more resources to both defense and vegetative
520 growth; thus, higher levels of expression of both the gibberellin and jasmonic acid pathways in
521 coastal plant leaves are consistent with this model. The major trade-off in this system is with
522 reproduction, for which the inland annual *M. guttatus* plants typically allocate more resources to
523 reproduction over vegetative growth and resistance to insect herbivores (Hall & Willis 2006;
524 Lowry et al. 2008; Hall et al. 2010; Baker & Diggle 2011; Baker et al. 2012; Holeski et al. 2013;
525 Lowry et al. 2019). By allocating resources to reproduction, annual plants can successfully
526 escape the terminal end-of-season drought that characterizes summers in western North America.
527 In contrast, perennial *M. guttatus* plants preferentially allocate resources to vegetative growth

528 and resistance to insect herbivores (Holeski et al. 2013; Lowry et al. 2019; Blanchard et al.
529 2024). The consistently lower temperatures and summer fog along the Pacific coast of North
530 America (Gilliam 2002; Garcia-Reyes & Largier 2012) provide conditions that facilitate a
531 perennial life history and, thus, this pattern of resource allocation.
532
533 While gibberellin biosynthesis and activity may be lower in inland plants than coastal plants at
534 the level of leaves, this pattern is likely reversed for the region of the shoot apex, where major
535 developmental patterns are laid down. Recent studies in this system have found that growth
536 architecture of coastal plants undergoes greater changes after the application of bioactive
537 gibberellin (GA3; Lowry et al. 2019). Furthermore, multiple studies suggest that the GA
538 biosynthesis gene *GA20ox2* plays a critical role in the divergence of the coastal perennial and
539 inland annual ecotypes (Gould et al. 2017; Kollar et al. 2025). *GA20ox2* is an allele frequency
540 outlier between coastal and inland populations (Gould et al. 2017) and is located within the
541 locally adaptive chromosome inversion that drives much of the divergence between the coastal
542 and inland ecotypes (Lowry & Willis 2010; Friedman 2014; Blanchard et al. 2024). *GA20ox2* is
543 expressed at a higher level in the shoot apices of inland plants than coastal plants (Kollar et al.
544 2025). We are currently conducting functional tests with this gene to determine whether it
545 contributes to the developmental signal that drives morphological divergence between the
546 ecotypes (Stanley & Lowry, 2024).
547
548 Beyond the jasmonic acid and gibberellin pathways, our study suggests the possible involvement
549 of the auxin hormone pathway in the divergence of the ecotypes. While not a significant
550 enrichment, eight of the auxin genes that we *a priori* identified were highly differentially

551 expressed between the ecotypes. Further, auxin was implicated in three of the modules in the
552 network analyses (tan, cyan, and greenyellow). In contrast, jasmonic acid and gibberellin were
553 only clearly implicated in the tan module, which appears to primarily capture gene expression
554 differences between leaf and bud stages, rather than divergence between the ecotypes (Fig. S11).
555 With both the cyan and greenyellow modules highly differentiated between the ecotypes, the
556 core role for auxin should be considered in future studies. Of particular interest is the ortholog of
557 *Amidase 1* (Migut.F01717), which mediates growth and stress responses by converting indole-3-
558 acetamide to the bioactive auxin (Pérez-Alonso et al., 2021). As a member of the greenyellow
559 module, this *Amidase 1* ortholog may play a key role in the differences in stress responses in
560 sulfur metabolism for coastal and inland ecotypes, as well as differences key physiological traits.
561 Sulfur metabolism can play a critical role in plant resilience (Takahashi et al., 2023) and has
562 previously been shown to differ in concentration between leaves of coastal and inland *M.*
563 *guttatus* plants (Lowry et al., 2012).
564
565 While the evolution of prostrate coastal ecotypes is a common pattern across plant species,
566 whether shifts in hormone pathways play an integral role in the evolution of ecotypes is still
567 unresolved. The only other system we know where appreciable progress has been made in
568 understanding this type of ecotype divergence is between headland and dune ecotypes of *Senecio*
569 *lautus*, where ethylene, gibberelins, and especially auxin have been implicated (James et al.
570 2021a,b; Wilkinson et al. 2021; Broad et al. 2024). No gene in either *S. lautus* or *M. guttatus* has
571 yet been confirmed to be involved in coastal ecotype divergence through functional genetic
572 studies.
573

574 Our global gene network expression analysis using WGCNA yielded additional insights into the
575 pathways that differ between ecotypes and across developmental stages. Interestingly, this
576 network analysis alone would have resulted in a different interpretation than our candidate
577 pathway analysis. While the gene network analyses captured new pathways to consider for
578 divergence between the ecotypes, as well as through development, it did not capture the same
579 insights about hormone pathway divergence. The main new insight into coastal and inland
580 ecotype divergence from our study was the recognition that gene regulation may greatly differ in
581 genes that control microscopic phenotypes, including vesicle trafficking and cell death
582 regulation. These microscopic processes likely serve as a critical intermediate between the
583 ultimately causative genetic variation at the DNA sequence level and phenotypic variation at the
584 organismal level. Another major insight from the network analysis was that there were major
585 differences in the regulation of photosynthetic processes between leaf and bud tissues, but not
586 between the ecotypes, as represented by the blue module (Fig. 6b). This finding suggests that the
587 natural variation in components of the photosynthetic machinery is likely not important for the
588 evolution of these coastal and inland ecotypes. Natural variation in photosynthetic efficiency has
589 been observed in other systems (Sharwood et al. 2022; Theeuwen et al. 2022), but it remains
590 unclear whether this is due to functional allelic variation within the photosynthetic machinery
591 itself or if it is caused by variation in genes peripheral to the core machinery.
592

593 **Salt spray adaptations of the coastal perennial ecotype**

594 Oceanic salt spray plays a key role in the local adaptation of coastal plant populations, leading to
595 the evolution of morphological, phenological, and physiological traits (Boyce 1954; Ahmad &
596 Wainwright 1976; Popovic & Lowry 2020; Itoh et al. 2021, 2024). While salt spray is important

597 for coastal population adaptations, the mechanisms underlying adaptations to this stress are
598 poorly understood (Du & Hesp 2020). In *M. guttatus*, we have previously demonstrated that
599 coastal perennials have higher tolerance to salt spray than inland annuals (Lowry et al. 2008,
600 2009; Popovic & Lowry 2020; Toll et al. 2024).
601
602 Salt spray adaptations likely share some mechanisms with soil salinity adaptations, especially in
603 terms of leaf tissue tolerance (Munn & Tester 2008). Leaf tissue tolerance to high sodium
604 accumulation is generally thought to involve the transport of sodium ions across cellular and
605 vacuolar membranes to maintain cellular homeostais, which includes genes in the SOS pathway
606 (Fig. 3; Ji et al. 2013; Yang & Guo 2018; Yin et al. 2020). The upregulation of *CIPK8* and *SOS1*
607 in coastal plants (Fig. 3, 4) is consistent with sodium being pumped out of the cytoplasm cells
608 into the apoplastic flow. The only other major cellular sodium homeostasis gene that was
609 significantly differentially expressed between the ecotypes was *HKT1*, which was also
610 upregulated in coastal plants and serves the function of importing sodium into the cytoplasm
611 from the apoplast. These seemingly contradictory patterns of gene expression suggest that coastal
612 plant cells are both exporting and importing sodium at higher rates than inland plants. However,
613 this result may be explained by our RNA-seq data being quantified across entire leaves. The
614 regulation and functions of *HKT* genes across different tissues are known to be complex (Munns
615 & Tester 2008; Zamani Babgohari et al. 2014; Gholizadeh et al. 2024). Thus, it is possible that
616 some coastal plant cells export sodium, while others take it up in a manner that maintains overall
617 leaf homeostasis. With single-cell sequencing, it may be possible in subsequent studies to test the
618 hypothesis that sodium is being actively partitioned between cells to maintain overall leaf
619 homeostasis (Li et al. 2024).

620

621 In addition to the core cellular sodium homeostasis genes, shifts in hormone levels can confer
622 adaptations to salt. Recent studies have found that both the jasmonic acid and gibberellin
623 pathways can alter salt tolerance in plants, although in inconsistent ways. Context matters, as
624 some studies have found that jasmonic acid can improve salt tolerance (reviewed in Khan et al.
625 2025), while others have found that it can make plants more susceptible to salt stress (Song et al.
626 2021). Context also appears to matter in the case of gibberellin, where the addition of this
627 hormone generally confers higher tolerance to soil salinity (Iqbal & Ashraf 2013; Farooq et al.
628 2022; Liu et al. 2023), but, in contrast, makes *M. guttatus* plants more susceptible to oceanic salt
629 spray in the field (Toll et al. 2024).

630

631 **Towards a general understanding of plant ecotype formation**

632 Ecotypes are thought to represent an important early stage in the process of speciation (reviewed
633 in Lowry 2012; Stankowski & Ravinet 2021; Butlin & Faria 2024). While most ecotypes will
634 likely not go on to become new species, it is important to understand their formation as part of
635 the speciation process, as some of them will complete the speciation process. The divergence of
636 inland and coastal populations have served as an excellent model for understanding the
637 speciation process, all the way back to when studies on them were used to coin the term
638 "ecotype" in the first place (Turesson 1922a). Our study provides further evidence that the
639 evolutionary divergence of hormone networks is a key component in the formation of locally
640 adapted ecotypes. We hypothesize that such shifts in the complex hormone networks drive the
641 evolution of shifts from perennality to annuality (Friedman 2020; Lundgren & Des Marais 2020)
642 and the accumulation of both extrinsic and intrinsic reproductive isolation. Indeed, a recent study

643 of headland and dune ecotypes of *S. latifolius* found that the evolutionary shifts in the auxin
644 network associated with different levels of gravitropism of the ecotypes may also cause hybrid
645 sterility (Wilkinson et al. 2021). Ultimately, functional studies of key candidate genes, currently
646 underway, will be necessary to test the hypothesis that changes in the regulation of hormone
647 pathways directly lead to the formation of ecotypes.
648

649 **Acknowledgments**

650 This work was supported by grants (IOS-1855927, IOS-2153100) from the National Science
651 Foundation and start-up funds from Michigan State University. We thank Madison Plunkert,
652 Lauren Stanley, Joanna Feehan, Colette Berg, Daniel Ortiz-Barrientos, and two anonymous
653 reviewers for comments that greatly helped improve this document.
654

655 **REFERENCES**

656 Aerts, N., Pereira Mendes, M., & Van Wees, S. C. M. (2021). Multiple levels of crosstalk in hormone
657 networks regulating plant defense. The Plant Journal: For Cell and Molecular Biology, 105(2), 489–
658 504.
659 Abrams, L. (1951). Illustrated Flora of the Pacific States, Vol. III, Geraniaceae to Scrophulariaceae.
660 Stanford University Press, Stanford, CA, USA.
661 Ahmad, I., & Wainwright, S. I. (1976). Ecotype differences in leaf surface properties of Agrostis
662 stolonifera from salt marsh, spray zone and inland habitats. New Phytologist, 76(2), 361–366.
663 Anders, S., Pyl, P. T., & Huber, W. (2015). HTSeq--a Python framework to work with high-throughput
664 sequencing data. Bioinformatics (Oxford, England), 31(2), 166–169.

Baker, R. L., & Diggle, P. K. (2011). Node-specific branching and heterochronic changes underlie population-level differences in Mimulus guttatus (Phrymaceae) shoot architecture. American Journal of Botany, 98(12), 1924–1934.

Baker, R. L., Hileman, L. C., & Diggle, P. (2012). Patterns of shoot architecture in locally adapted populations are linked to intraspecific differences in gene regulation. The New Phytologist, 196(1), 271–281.

Blanchard, M. L., Lowry, D. B., & Holeski, L. M. (2024). Patterns of constitutive and induced herbivore defence are complex, but share a common genetic basis in annual and perennial monkeyflower. Functional Ecology, 38(8), 1796–1810.

Boyce, S. G. (1954). The salt spray community. Ecological Monographs, 24(1), 29–67.

Broad, Z., Lefreve, J., Wilkinson, M. J., Barton, S., Barbier, F., Jung, H., Donovan, D., & Ortiz-Barrientos, D. (2024). Gravitropic gene expression divergence associated with adaptation to contrasting environments in an Australian wildflower. Molecular Ecology, e17543.

Butlin, R. K., & Faria, R. (2024). Local adaptation and reproductive isolation: when does speciation start? Evolutionary Journal of the Linnean Society, 3(1). https://doi.org/10.1093/evolinnean/kzae003

Clausen, J., Keck, D. D., & Hiesey, W. M. (1940). Experimental studies on the nature of species. I. Effect of varied environments on western North American plants. Carnegie Institution of Washington Publication No. 520.

Clausen, J., Keck, D. D., & Hiesey, W. M. (1948). Experimental studies on the nature of species. III. Environmental responses of climatic races of Achillea. Carnegie Institution of Washington Publication No. 581.

Claus Wasternack. (2017). A plant?s balance of growth and defense ? revisited. The New Phytologist, 215(4), 1291–1294.

Coyne, J. A., & Orr, H. A. (2004). Speciation. Sinauer Associates.

Depuydt, S., & Hardtke, C. S. (2011). Hormone signalling crosstalk in plant growth regulation. Current Biology: CB, 21(9), R365–R373.

691 Du, J., & Hesp, P. A. (2020). Salt Spray Distribution and Its Impact on Vegetation Zonation on Coastal
692 Dunes: a Review. Estuaries and Coasts, 43(8), 1885–1907.
693 Farooq, M., Khan, M. A., Zhao, D.-D., Asif, S., Kim, E.-G., Jang, Y.-H., Park, J.-R., Lee, I.-J., & Kim,
694 K.-M. (2022). Extrinsic role of gibberellin mitigating salinity effect in different rice genotypes.
695 Frontiers in Plant Science, 13, 1041181.
696 Foster, S. A., McKinnon, G. E., Steane, D. A., Potts, B. M., & Vaillancourt, R. E. (2007). Parallel
697 evolution of dwarf ecotypes in the forest tree Eucalyptus globulus. The New Phytologist, 175(2),
698 370–380.
699 Friedman, J. (2014). Genetic determinants and epistasis for life history trait differences in the common
700 monkeyflower, Mimulus guttatus. The Journal of Heredity, 105(6), 816–827.
701 Friedman, J. (2020). The evolution of annual and perennial plant life histories: Ecological correlates and
702 genetic mechanisms. Annual Review of Ecology, Evolution, and Systematics, 51(1), 461–481.
703 Fujita, M., Fujita, Y., Noutoshi, Y., Takahashi, F., Narusaka, Y., Yamaguchi-Shinozaki, K., & Shinozaki,
704 K. (2006). Crosstalk between abiotic and biotic stress responses: a current view from the points of
705 convergence in the stress signaling networks. Current Opinion in Plant Biology, 9(4), 436–442.
706 García-Reyes, M., & Largier, J. L. (2012). Seasonality of coastal upwelling off central and northern
707 California: New insights, including temporal and spatial variability. Journal of Geophysical Research,
708 117(C3). https://doi.org/10.1029/2011jc007629
709 Gasperini, D., & Howe, G. A. (2024). Phytohormones in a universe of regulatory metabolites: lessons
710 from jasmonate. Plant Physiology, 195(1), 135–154.
711 Gholizadeh, F., Mirmazloum, I., & Janda, T. (2024). Genome-wide identification of HKT gene family in
712 wheat (Triticum aestivum L.): Insights from the expression of multiple genes (HKT, SOS, TVP and
713 NHX) under salt stress. Plant Stress, 13(100539), 100539.
714 Gilliam, H. (2002). Weather of the San Francisco Bay Region. University of California Press.

715 Gould, B. A., Chen, Y., & Lowry, D. B. (2017). Pooled ecotype sequencing reveals candidate genetic
716 mechanisms for adaptive differentiation and reproductive isolation. Molecular Ecology, 26(1), 163–
717 177.
718 Gould, B. A., Chen, Y., & Lowry, D. B. (2018). Gene regulatory divergence between locally adapted
719 ecotypes in their native habitats. Molecular Ecology, 27(21), 4174–4188.
720 Guo, Q., Major, I. T., & Howe, G. A. (2018). Resolution of growth-defense conflict: mechanistic insights
721 from jasmonate signaling. Current Opinion in Plant Biology, 44, 72–81.
722 Hall, M. C., Basten, C. J., & Willis, J. H. (2006). Pleiotropic quantitative trait loci contribute to
723 population divergence in traits associated with life-history variation in Mimulus guttatus. Genetics,
724 172(3), 1829–1844.
725 Hall, M. C., Lowry, D. B., & Willis, J. H. (2010). Is local adaptation in Mimulus guttatus caused by trade-
726 offs at individual loci? Molecular Ecology, 19(13), 2739–2753.
727 Hall, M. C., & Willis, J. H. (2006). Divergent selection on flowering time contributes to local adaptation
728 in Mimulus guttatus populations. Evolution; International Journal of Organic Evolution, 60(12),
729 2466–2477.
730 Havko, N. E., Major, I. T., Jewell, J. B., Attaran, E., Browse, J., & Howe, G. A. (2016). Control of carbon
731 assimilation and partitioning by jasmonate: An accounting of growth-defense tradeoffs. Plants, 5(1),
732 7.
733 Hellsten, U., Wright, K. M., Jenkins, J., Shu, S., Yuan, Y., Wessler, S. R., Schmutz, J., Willis, J. H., &
734 Rokhsar, D. S. (2013). Fine-scale variation in meiotic recombination in Mimulus inferred from
735 population shotgun sequencing. Proceedings of the National Academy of Sciences of the United
736 States of America, 110(48), 19478–19482.
737 Hitchcock, C. L., Cronquit, A. (1973). Flora of the Pacific Northwest: an illustrated manual. University of
738 Washington Press. Seattle, WA, USA.
739 Howe, G. A., Major, I. T., & Koo, A. J. (2018). Modularity in jasmonate signaling for multistress
740 resilience. Annual Review of Plant Biology, 69, 387–415.

741 Iqbal, M., & Ashraf, M. (2013). Gibberellic acid mediated induction of salt tolerance in wheat plants:
742 Growth, ionic partitioning, photosynthesis, yield and hormonal homeostasis. Environmental and
743 Experimental Botany, 86, 76–85.
744 Itoh, M. (2021). Phenotypic variation and adaptation in morphology and salt spray tolerance in coastal
745 and inland populations of Setaria viridis in central Japan. Weed Research, 61(3), 199–209.
746 Itoh, M., Fukunaga, K., & Osako, T. (2024). Local adaptation in parapatric and sympatric mosaic coastal
747 habitats through trait divergence of Setaria viridis. The Journal of Ecology.
748 https://doi.org/10.1111/1365-2745.14269
749 James, M. E., Allsopp, R. N., Groh, J. S., Kaur, A., Wilkinson, M. J., & Ortiz-Barrientos, D. (2023).
750 Uncovering the genetic architecture of parallel evolution. Molecular Ecology, 32(20), 5575–5589.
751 James, M. E., Wilkinson, M. J., Bernal, D. M., Liu, H., North, H. L., Engelstädter, J., & Ortiz-Barrientos,
752 D. (2021). Phenotypic and genotypic parallel evolution in parapatric ecotypes of Senecio. Evolution;
753 International Journal of Organic Evolution, 75(12), 3115–3131.
754 Ji, H., Pardo, J. M., Batelli, G., Van Oosten, M. J., Bressan, R. A., & Li, X. (2013). The Salt Overly
755 Sensitive (SOS) pathway: established and emerging roles. Molecular Plant, 6(2), 275–286.
756 Kazan, K., & Manners, J. M. (2012). JAZ repressors and the orchestration of phytohormone crosstalk.
757 Trends in Plant Science, 17(1), 22–31.
758 Kollar, L. M., Stanley, L. E., Kenchanmane Raju, S. K., Lowry, D. B., & Niederhuth, C. E. (2025). The
759 evolution of locally adaptive chromosome inversions in Mimulus guttatus. Molecular Ecology,
760 e17708.
761 Koo, A. J., Thireault, C., Zemelis, S., Poudel, A. N., Zhang, T., Kitaoka, N., Brandizzi, F., Matsuura, H.,
762 & Howe, G. A. (2014). Endoplasmic reticulum-associated inactivation of the hormone jasmonoyl-L-
763 isoleucine by multiple members of the cytochrome P450 94 family in Arabidopsis. The Journal of
764 Biological Chemistry, 289(43), 29728–29738.
765 Langfelder, P., & Horvath, S. (2008). WGCNA: an R package for weighted correlation network analysis.
766 BMC Bioinformatics, 9(1), 559.

767 Law, C. W., Chen, Y., Shi, W., & Smyth, G. K. (2014). voom: Precision weights unlock linear model
768 analysis tools for RNA-seq read counts. Genome Biology, 15(2), R29.
769 Li, H. (2013). Aligning sequence reads, clone sequences and assembly contigs with BWA-MEM. In
770 arXiv [q-bio.GN]. arXiv. http://arxiv.org/abs/1303.3997
771 Li, H., Handsaker, B., Wysoker, A., Fennell, T., Ruan, J., Homer, N., Marth, G., Abecasis, G., Durbin, R.,
772 & 1000 Genome Project Data Processing Subgroup. (2009). The Sequence Alignment/Map format
773 and SAMtools. Bioinformatics (Oxford, England), 25(16), 2078–2079.
774 Li, P., Liu, Q., Wei, Y., Xing, C., Xu, Z., Ding, F., Liu, Y., Lu, Q., Hu, N., Wang, T., Zhu, X., Cheng, S.,
775 Li, Z., Zhao, Z., Li, Y., Han, J., Cai, X., Zhou, Z., Wang, K., … Peng, R. (2024). Transcriptional
776 landscape of cotton roots in response to salt stress at single-cell resolution. Plant Communications,
777 5(2), 100740.
778 Liu, J., Wu, Y., Dong, G., Zhu, G., & Zhou, G. (2023). Progress of research on the physiology and
779 molecular regulation of sorghum growth under salt stress by gibberellin. International Journal of
780 Molecular Sciences, 24(7), 6777.
781 Lohman, B. K., Weber, J. N., & Bolnick, D. I. (2016). Evaluation of TagSeq, a reliable low-cost
782 alternative for RNAseq. Molecular Ecology Resources, 16(6), 1315–1321.
783 Love, M. I., Huber, W., & Anders, S. (2014). Moderated estimation of fold change and dispersion for
784 RNA-seq data with DESeq2. Genome Biology, 15(12), 550.
785 Lowry, D. B., Hall, M. C., Salt, D. E., & Willis, J. H. (2009). Genetic and physiological basis of adaptive
786 salt tolerance divergence between coastal and inland Mimulus guttatus. The New Phytologist, 183(3),
787 776–788.
788 Lowry, D. B., Rockwood, R. C., & Willis, J. H. (2008). Ecological reproductive isolation of coast and
789 inland races of Mimulus guttatus. Evolution; International Journal of Organic Evolution, 62(9), 2196–
790 2214.

Lowry, D. B., Sheng, C. C., Zhu, Z., Juenger, T. E., Lahner, B., Salt, D. E., & Willis, J. H. (2012). Mapping of ionomic traits in Mimulus guttatus reveals Mo and Cd QTLs that colocalize with MOT1 homologues. PloS One, 7(1), e30730.

Lowry, D. B., & Willis, J. H. (2010). A widespread chromosomal inversion polymorphism contributes to a major life-history transition, local adaptation, and reproductive isolation. PLoS Biology, 8(9). https://doi.org/10.1371/journal.pbio.1000500

Lundgren, M. R., & Des Marais, D. L. (2020). Life history variation as a model for understanding trade-offs in plant-environment interactions. Current Biology: CB, 30(4), R180–R189.

Martin, M. (2011). Cutadapt removes adapter sequences from high-throughput sequencing reads. EMBnet.journal, 17, 10–12.

Marx, H. E., Scheidt, S., Barker, M. S., & Dlugosch, K. M. (2020). TagSeq for gene expression in non-model plants: A pilot study at the Santa Rita Experimental Range NEON core site. Applications in Plant Sciences, 8(11), e11398.

Meyer, E., Aglyamova, G. V., & Matz, M. V. (2011). Profiling gene expression responses of coral larvae (Acropora millepora) to elevated temperature and settlement inducers using a novel RNA-Seq procedure. Molecular Ecology, 20(17), 3599–3616.

Murphy, A. (2015). Hormone crosstalk in plants. Journal of Experimental Botany, 66, 4853–4854.

Nagy, E. S., & Rice, K. J. (1997). Local adaptation in two subspecies of an annual plant: Implications for migration and gene flow. Evolution; International Journal of Organic Evolution, 51(4), 1079–1089.

Nesom, G. L. (2012). Taxonomy of Erythranthe sect. Simiola (Phrymaceae) in the USA and Mexico. Phytoneuron 2012-40:1-123.

Pérez-Alonso, M.-M., Ortiz-García, P., Moya-Cuevas, J., Lehmann, T., Sánchez-Parra, B., Björk, R. G., Karim, S., Amirjani, M. R., Aronsson, H., Wilkinson, M. D., & Pollmann, S. (2021). Endogenous indole-3-acetamide levels contribute to the crosstalk between auxin and abscisic acid, and trigger plant stress responses in Arabidopsis. Journal of Experimental Botany, 72(2), 459–475.

816 Pieterse, C., Pierik, R., & Van Wees, S. C. M. (2014). Different shades of JAZ during plant growth and
817 defense. The New Phytologist, 204(2), 261–264.
818 Popovic, D., & Lowry, D. B. (2020). Contrasting environmental factors drive local adaptation at opposite
819 ends of an environmental gradient in the yellow monkeyflower (Mimulus guttatus). American Journal
820 of Botany, 107(2), 298–307.
821 Robinson, M. D., McCarthy, D. J., & Smyth, G. K. (2010). edgeR: a Bioconductor package for
822 differential expression analysis of digital gene expression data. Bioinformatics (Oxford, England),
823 26(1), 139–140.
824 Roda, F., Ambrose, L., Walter, G. M., Liu, H. L., Schaul, A., Lowe, A., Pelser, P. B., Prentis, P.,
825 Rieseberg, L. H., & Ortiz-Barrientos, D. (2013). Genomic evidence for the parallel evolution of
826 coastal forms in the Senecio lautus complex. Molecular Ecology, 22(11), 2941–2952.
827 Schemske, D. (2000). Understanding the origin of species. Evolution, 54(3), 1069–1073.
828 Sharwood, R. E., Quick, W. P., Sargent, D., Estavillo, G. M., Silva-Perez, V., & Furbank, R. T. (2022).
829 Mining for allelic gold: finding genetic variation in photosynthetic traits in crops and wild relatives.
830 Journal of Experimental Botany, 73(10), 3085–3108.
831 Sobel, J. M. (2014). Ecogeographic isolation and speciation in the genus Mimulus. The American
832 Naturalist, 184(5), 565–579.
833 Sobel, J. M., Chen, G. F., Watt, L. R., & Schemske, D. W. (2010). The biology of speciation. Evolution;
834 International Journal of Organic Evolution, 64(2), 295–315.
835 Stankowski, S., & Ravinet, M. (2021). Defining the speciation continuum. Evolution; International
836 Journal of Organic Evolution, 75(6), 1256–1273.
837 Takahashi, H., Marsolais, F., Cuypers, A., & Kopriva, S. (2023). Sulfur metabolism: actions for plant
838 resilience and environmental adaptation. Journal of Experimental Botany, 74(11), 3271–3275.
839 Theeuwen, T. P. J. M., Logie, L. L., Harbinson, J., & Aarts, M. G. M. (2022). Genetics as a key to
840 improving crop photosynthesis. Journal of Experimental Botany, 73(10), 3122–3137.

Toll, K., Blanchard, M., Scharnagl, A., Holeski, L. M., & Lowry, D. B. (2024). Plant hormone manipulation impacts salt spray tolerance, which preempts herbivory as a driver of local adaptation in the yellow monkeyflower,Mimulus guttatus. In bioRxiv (p. 2024.05.23.595619). https://doi.org/10.1101/2024.05.23.595619

Turesson, G. (1922a). The species and the variety as ecological units. Hereditas, 3(1), 100–113.

Turesson, G. (1922b). The genotypical response of the plant species to the habitat. Hereditas 3(3): 211–350.

Twyford, A. D., & Friedman, J. (2015). Adaptive divergence in the monkey flower Mimulus guttatus is maintained by a chromosomal inversion: GENETICS OF ADAPTIVE DIVERGENCE IN MONKEY FLOWERS. Evolution; International Journal of Organic Evolution, 69(6), 1476–1486.

Twyford, A. D., Streisfeld, M. A., Lowry, D. B., & Friedman, J. (2015). Genomic studies on the nature of species: adaptation and speciation inMimulus. In Molecular Ecology (Vol. 24, Issue 11, pp. 2601–2609). https://doi.org/10.1111/mec.13190

van Kleunen, M. (2007). Adaptive genetic differentiation in life-history traits between populations of Mimulus guttatus with annual and perennial life-cycles. Evolutionary Ecology, 21(2), 185–199.

VanWallendael, A., Soltani, A., Emery, N. C., Peixoto, M. M., Olsen, J., & Lowry, D. B. (2019). A molecular view of plant local adaptation: Incorporating stress-response networks. Annual Review of Plant Biology, 70(1), 559–583.

Verhoeven, K. J. F., Poorter, H., Nevo, E., & Biere, A. (2008). Habitat-specific natural selection at a flowering-time QTL is a main driver of local adaptation in two wild barley populations. Molecular Ecology, 17(14), 3416–3424.

Vickery, R. K., Jr. (1978). Case studies in the evolution of species complexes in Mimulus. In Evolutionary Biology (pp. 405–507). Springer, USA.

Voesenek, L. A. C. J., & Blom, C. W. P. M. (1996). Plants and Hormones: An Ecophysiological View on Timing and Plasticity. The Journal of Ecology, 84(1), 111.

866 Weng, X., & Juenger, T. E. (2022). A high-throughput 3'-tag RNA sequencing for large-scale time-series
867 transcriptome studies. Methods in Molecular Biology (Clifton, N.J.), 2398, 151–172.
868 Wilkinson, M. J., Roda, F., Walter, G. M., James, M. E., Nipper, R., Walsh, J., Allen, S. L., North, H. L.,
869 Beveridge, C. A., & Ortiz-Barrientos, D. (2021). Adaptive divergence in shoot gravitropism creates
870 hybrid sterility in an Australian wildflower. Proceedings of the National Academy of Sciences of the
871 United States of America, 118(47), e2004901118.
872 Yang, D.-L., Yao, J., Mei, C.-S., Tong, X.-H., Zeng, L.-J., Li, Q., Xiao, L.-T., Sun, T.-P., Li, J., Deng, X.-
873 W., Lee, C. M., Thomashow, M. F., Yang, Y., He, Z., & He, S. Y. (2012). Plant hormone jasmonate
874 prioritizes defense over growth by interfering with gibberellin signaling cascade. Proceedings of the
875 National Academy of Sciences of the United States of America, 109(19), E1192–E1200.
876 Yang, Y., & Guo, Y. (2018). Elucidating the molecular mechanisms mediating plant salt-stress responses.
877 The New Phytologist, 217(2), 523–539.
878 Yin, X., Xia, Y., Xie, Q., Cao, Y., Wang, Z., Hao, G., Song, J., Zhou, Y., & Jiang, X. (2020). The protein
879 kinase complex CBL10-CIPK8-SOS1 functions in Arabidopsis to regulate salt tolerance. Journal of
880 Experimental Botany, 71(6), 1801–1814.
881 Zamani Babgohari, M., Ebrahimie, E., & Niazi, A. (2014). In silico analysis of high affinity potassium
882 transporter (HKT) isoforms in different plants. Aquatic Biosystems, 10(1), 9.
883 Züst, T., & Agrawal, A. A. (2017). Trade-offs between plant growth and defense against insect herbivory:
884 An emerging mechanistic synthesis. Annual Review of Plant Biology, 68(1), 513–534.

885 **Data Accessibility and Benefit-Sharing**

886 Raw sequence reads and processed count data are publicly available and accessible for reuse
887 through the NCBI Gene Expression Omnibus (GEO) under accession numbers GSE280929 and
888 GSM8607613-GSM8607692. Custom scripts for analysis can be found on GitHub at
889 https://github.com/lowrylab/Mimulus_expression_across_development

890 **Author contributions**

891 DBL and YC designed the experiment. YC conducted the experiment, performed RNA extractions,
892 and prepared the genomic libraries. JDO, BAG, and DBL conducted the data analyses. DBL and
893 JDO wrote the manuscript, with input from YC and BAG.

894 **Supporting/Supplementary information**

895 Additional supporting information can be found online in the Supporting Information section and
896 includes the following:

897 **Supplementary Methods**

898 **Supplementary Figures S1-S27**

899 **Supplementary Data Files**